Rainfall-induced slope failure in Northland Allochthon formation

S.J. Harris & R.P. Orense
Department of Civil & Environmental Engineering, University of Auckland, Auckland, New Zealand, shar228@aucklanduni.ac.nz, r.orense@auckland.ac.nz

K. Itoh
National Institute of Occupational Safety and Health, Tokyo, Japan, k-ito@s.jniosh.go.jp

ABSTRACT: During the winter season of 2008, a section of the roadway embankment adjacent to State Highway 1 in Silverdale, New Zealand, collapsed as a result of heavy rainfall. The failure occurred in a cut slope through the landslide-prone Northland Allochthon formation. To investigate the response of this formation to rainwater infiltration, volumetric water content transducers and a rainfall gauge were installed through a cross section 45 meters away from and parallel to the failed slope and during the winter period of 2010, monitoring was performed. Saturated/unsaturated seepage analyses were then conducted to simulate the variation in the monitored volumetric water contents. After modeling the hydraulic properties, slope stability analysis was conducted to investigate the failed slope. This paper presents the partial results of the ongoing monitoring of the slope and the attempt to simulate the failure through seepage analysis and slope stability analysis.

KEYWORDS: Rainfall, slope failure, field monitoring, seepage analyses

1 INTRODUCTION

Various regions of New Zealand are susceptible to rainfall induced landslides. This is due to a combination of the precipitation patterns, the topography and the geotechnical characteristics of certain New Zealand soils. It can also be attributed to the change in land use of which many parts of New Zealand has undergone in the last 150 years (Brooks et al., 2002). In 2008, GNS Science recorded 313 significant landslides, most of which were triggered by rainstorms. These landslides caused damage at the cost of several million dollars (NIWA & G.N.S., 2009).

To understand these, landslides, field monitoring has been undertaken by various NZ researchers. Hawke & McConchie (2011), in particular, monitored an 'incipient' landslide in Hawke's Bay. In an effort to explain the failure mechanism of the site in relation to rainfall characteristics, they monitored the fluctuating volumetric water content of the soil and its piezometric response to recorded rainfall events over a 5 year-period. Another similar study was undertaken by Zhan et al. (2007), who used tensiometers, moisture probes and a vee-notch flow meter to record the runoff from a naturally grassed slope.

In an effort to mitigate the cost of such landslides, a site-specific landslide warning system is being developed by the authors for a site which experienced a landslide in the winter of 2008. Field monitoring consisting of volumetric water content sensors to record the fluctuating water content of the soil due to precipitation events, recorded using a tipping bucket rain-gauge, was undertaken. 2D finite element modelling (FEM) was used to replicate this fluctuating water content due to rainfall events. A limit equilibrium analyses was performed at each time step in the FEM to determine the factor of safety (FOS) against slope failure. To calibrate these models, the 2008 rainfall data which caused a landslide at the site was used as an input into the models. If calibrated correctly, the model should approach a factor of safety close to unity at the same time as when the landslide occurred at the site. This method is hence a back analysis in which the pore-pressure/matric suction distribution at the time of failure is estimated using the actual rainfall data and permeability characteristics at the site. This paper presents the preliminary results of this calibration process. In the future, it is aimed to develop these computer models into a real time warning system.

2 SITE DESCRIPTION

The site, shown in Figure 1, is located in Silverdale, approximately 30 kilometres north of New Zealand's largest city, Auckland. It was formed from an 11m cut operation during the construction of State Highway One, which lies at the toe of the slope. This site was selected because of the effect a future landslide occurring at this site would have on the

roading network. Because the site is man-made, it is also linear along its length, making the 2D numerical modelling viable. The slope angle is approximately 15°, which is similar to many natural slopes in the region (O'Sullivan, 2009). A bench was formed at mid-height of the slope, with counterfort trench drains discharging onto a dish drain placed on this bench. A subsoil drain is located at the toe of the slope. The site is grassed, with a row of low height trees and shrubs present at mid-height of the slope. The soil at the site largely consists of Northland Allochthon residual soil.

Figure 1.The monitored site. The landslide occurred in the winter of 2008. State Highway 1 can be seen at the toe of the slope.

The Northland Allochthon soil group is well-known for its susceptibly to landsliding and creep, and the subsequent effect on engineering structures (O'Sullivan, 2009; Winkler, 2003). The susceptibility of this soil to landsliding arises from its low shear strength and low permeability, which results in a soil remaining nearly saturated all year long (Winkler, 2003). The original design reports for the site initially gave a factor of safety of approximately unity during periods of saturation, in large part due to the weak underlying Northland Allochthon residual soil (Tilsley, 1998). Unsurprisingly then, in the winter of 2008 (approximately 10 years after completion of State Highway One), a landslide occurred at the site following a series of rainfall events. This landslide almost crossed over into State Highway One, which could have had a disastrous effect on the Auckland roading network.

3 METHODOLOGY

Eight volumetric water content sensors were installed at 0.5m depth intervals to a total depth of 2m at two locations at the site. These sensors were placed along the same cross section of the site, approximately 45m from the existing landslide. The probes were installed by hand augering to the desired depth and using a PVC tube to push the sensors into the soil. The auger holes were backfilled and compacted following installation of the sensors. A tipping bucket rain gauge was installed at the site to monitor rainfall events. The SL5-1L data logger (ICT International), powered via a solar panel, recorded the data at 15 min intervals. The hourly rainfall record obtained at the site for 2010 was then input as an influx into FEM. The results of this finite element model were calibrated with the results obtained from the sensors. Once the model was calibrated, the 2008 hourly rainfall record which caused the landslide was input as an influx into the FEM. A limit equilibrium analyses was undertaken at each time step of this FEM as a means of verification. If the FEM was well-calibrated, the factor of safety should be at a minimum (close to unity) at the same time when failure occurred at the site.

3.1 *2008 Rainfall Data*

Because the field monitoring was not in progress during the 2008 rainfall events which caused the landslide, the 2008 hourly rainfall record was obtained from 3 nearby meteorological stations maintained by the National Institute of Water & Atmospheric Research (NIWA). The rainfall history at the site was estimated by calculating the weighted average of the rainfall data from the three stations based on the distance of the stations from the site.

3.2 *Computer modelling*

The software SEEP/W (GeoStudio) was used to undertake the FEM, in conjunction with SLOPE/W (Geostudio) for the limit equilibrium analyses. This software package allows the matric suction profile from the FEM to be directly imported into the limit equilibrium analyses.

The hourly rainfall record was applied as a unit influx into the FEM. The toe drain was modelled as having a constant total head (elevation head + piezometric head) equal to the elevation of the toe drain. Thus, it is assumed that this toe drain is capable of draining all water away from the site. It was assumed that the conterfort drains installed midway up the slope were derelict or ineffective. This assumption was based on the current condition of the pipes, and references made by Winkler (2003) to the ineffectiveness of such drainage systems in the low permeability soils of the Northland Allochthon. The boundary of the bottom of the model was defined as a no flow boundary, as well as the sides of the model (based on an assumption of symmetry). The model mesh was generated automatically into 1m square grids; however in the upper 2m of the model, this mesh was gradually refined into a 0.25m square grid in order to fully capture the advancement of the wetting front.

The grid and radius function was used to find the slip centre and the failure surface using SLOPE/W. The Morgenstern and Price method was used to evaluate the factor of safety of the slope at each time step in the FEM.

3.3 *Soil Properties*

Three soil layers were identified at the site: an upper alluvium layer (possibly a re-deposited Northland Allochthon), the completely weathered Northland Allochthon layer and a moderately weathered Northland Allochthon layer. The soil-water characteristic curve (SWCC) required for the saturated/unsaturated FEM was determined empirically. The SWCCs were estimated based on the grain size distributions, using the Arya and Paris method (Arya & Paris, 1981). The parameter α was assumed to be 1.1, as the soil is fine textured (Arya et al., 1982 as cited in Arya et al. 1999). It is noted that α is not constant, but varies along the suction range and because of the complexities of the development of matric suction, α should be estimated from experimental SWCC data, rather than as a geometric constant (Arya, et al., 1999). It is likely that the accuracy of the model is hence limited by these assumptions made. The SWCCs determined from this method (plotted with respect to the degree of saturation) are shown in Figure 2.

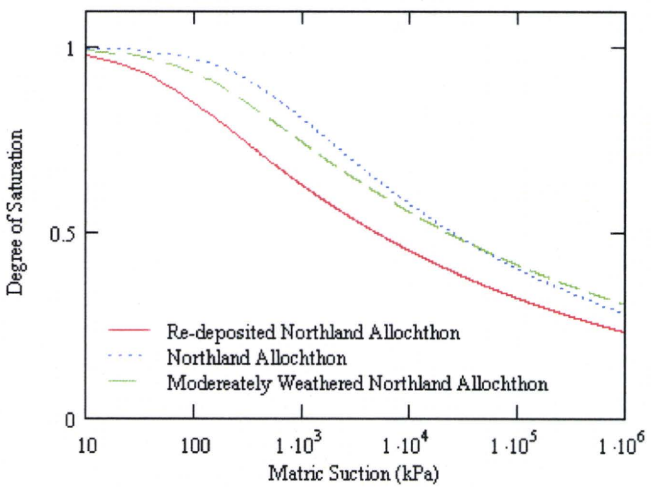

Figure 2. SWCCs obtained using the Arya & Paris method.

To model the permeability/matric suction relationship, the equation proposed by van Genuchten (1980) was fitted to these empirically derived equations. The saturated permeability and the van Genuchten parameters were then altered in the FEM until the model was in agreement with the field monitored results.

The shear strengths of the soil were initially obtained from those used in the original design. These shear strengths were obtained from a variety of back analyses, shear strength tests and experience with the soils within the region. These shear strength parameters adopted are shown in Table 1. The shear strength component due to matric suction was estimated based on Equation 1, as set out by Vanapalli et al. (1996).

$$\phi^b = \left[\left(\frac{\theta_w - \theta_r}{\theta_s - \theta_r} \right) \tan \phi' \right] \quad (1)$$

where ϕ^b is the angle of shearing resistance with respect to matric suction, ϕ' is the normal angle of shearing resistance, θ_w, θ_r and θ_s are the water content, saturated water content and residual water content (by volume) of the soil, respectively.

Table 1. Estimated shear strength parameters

Soil Type	γ (kN/m³)	c' (kPa)	Φ' (°)
Alluvium/re-deposited Allochthon	16	3	28
Completely weathered Northland Allochthon	17	0	17
Moderately weathered Allochthon	17	5	28

4 RESULTS AND DISCUSSION

Figure 3 shows the results obtained from the field monitoring during the winter months of 2010. The upper graph shows the hourly rainfall recorded at the site throughout the winter. Rainfall data obtained from the NIWA sites throughout the same period were overlaid on this plot to evaluate the accuracy of using the method described in Section 3.1. As observed, the two data are similar; thus, using the 2008 rainfall data obtained from the NIWA sites to simulate the 2008 landslide is plausible.

The first rainfall event observed was the first significant rainfall following a prolonged dry period. The middle graph depicts the volumetric water content (θ_w) of the shallow sensors (0.5m deep), and the lower graph shows the θ_w of the deeper sensors (approximately 1.5m deep).

4.1 *Shallow Sensors*

As observed, the water content at shallow depths fluctuates greatly with each rainfall event. The θ_w of the soil at both the mid-height of the slope (dashed line), and at the toe of the slope (solid line) increase rapidly during each significant rainfall event, often reaching full saturation (i.e., θ_w of approximately 38%) throughout the winter period. The θ_w at mid-height of the slope then recovers rapidly and almost immediately following each rainfall event. The soil at the toe of the slope however appears to stay saturated for a much longer period of time following the rainfall event. This is either due to a different SWCC, or due to the flow of water upslope of the

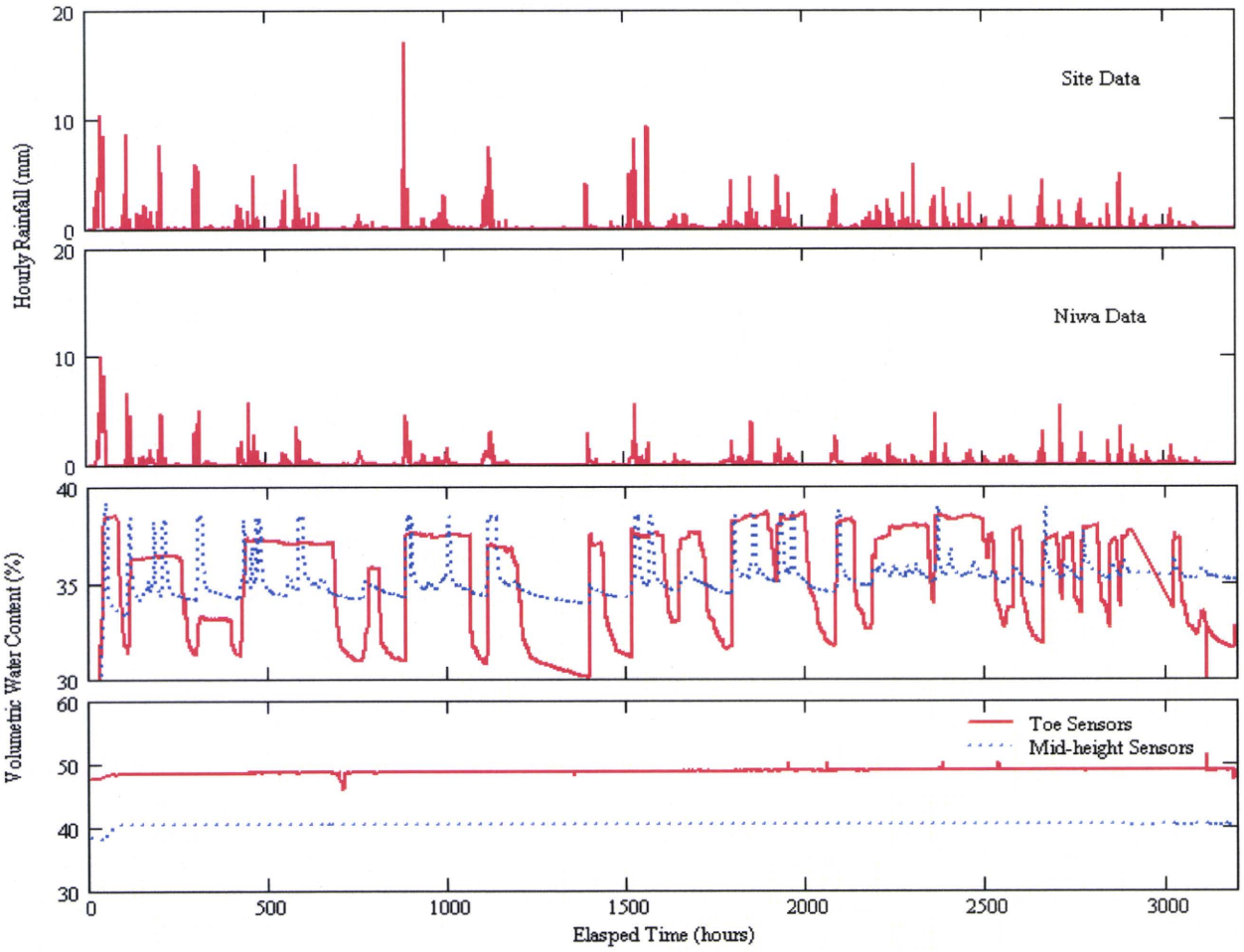

Figure 3. Results obtained from the field monitoring. Elapsed time = 0 corresponds to the 19th of May 2010.

sensors. Although initially the soil recovers very rapidly and linearly, once a certain θ_w is reached (approximately 34% for the mid-height sensor and 31% for the toe sensor), θ_w decreases at a diminishing rate, and as a result, the degree of saturation rarely drops below 80% for the entire winter period for these shallow sensors.

4.2 *Deep Sensors*

Referring to the deep sensors (bottom graph of Figure 3), apart from an initial increase in θ_w at the start of the monitoring period, the water content at this depth appeared to stay at a constant value for the entire winter. This indicates that the soil at this depth remains nearly saturated over the entire season.

These results are consistent with that described in the literature. Hawke & McConchie (2011) reported that the volumetric water content of the soil at 250mm deep fluctuated greatly at each significant rainfall event. At a 500mm depth, the fluctuations were more gradual, and at a depth of 1000mm the soil water content rarely fluctuated over an entire year. This is also consistent with the observations of O'Sullivan (2009) and Winkler (2003), who suggested that due to the low permeability of the soil, the water table remains high, and the soil fully saturated throughout the entire year. This explains why the water content at 1.5m deep rarely fluctuated throughout the monitoring period. The major fluctuations in the water content at the shallow soil could be due to a number of factors. The first is the installation of the sensors could have lead to localised cracks around the sensor location, thus increasing the local permeability. It could also be due to the roots of the vegetation at the site (which were recorded to an approximate depth of 500mm in hand augers undertaken) which allowed water to infiltrate into the soil more easily. The soil also experiences heavy shrink/swell movement, leading to large cracks, up to 30mm wide and 500mm thick occurring in dry periods. These explain why the soil at this shallow depth experiences a large increase in θ_w, regardless of the initial water content level. Because the landslide at the site occurred mid-winter, modelling the effect of such shrinkage cracking was ignored in this research. It is noted however that a study undertaken by Zhan et al. (2007) investigated the effects of rainfall infiltration on an expansive soil.

4.3 *Computer Modelling*

Figure 4 depicts the comparison between the FEM-calculated θ_w and the field-measured θ_w. The FEM was reasonably successful at replicating the fluctuating volumetric water content of the soil. While the general pattern is captured, there is still some discrepancy between the level of θ_w reached during each rainfall event, and also during the drying path of the soil. The discrepancy of the level of the θ_w

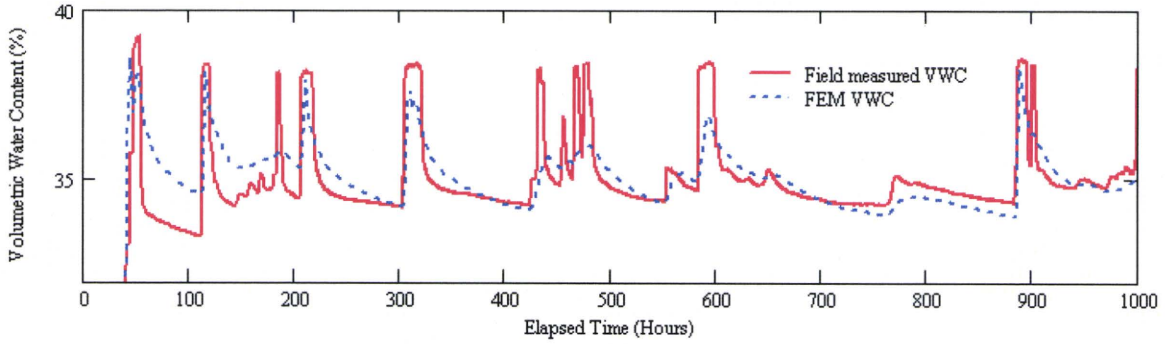

Figure 5. Comparison between the FEM θ_w and the field measured θ_w, for the sensor located 0.5m deep at mid-height of the slope. Elapsed time = 0 corresponds to the 19th of May 2010.

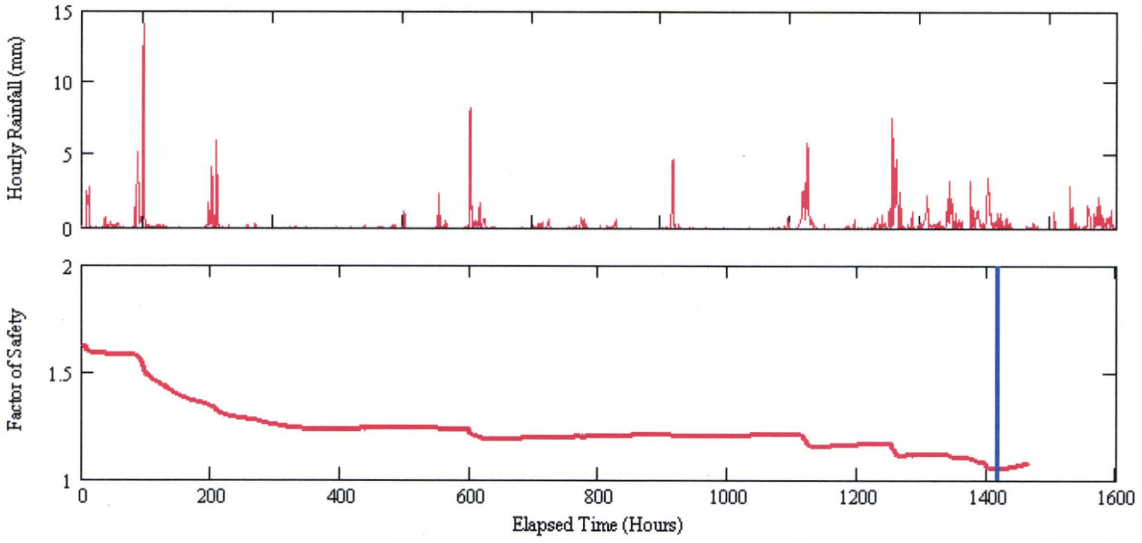

Figure 4. 2008 hourly rainfall (upper graph), and corresponding factor of safety. Elapsed time = 0 corresponds to the 1st of May 2008. The vertical line represents the approximate elapsed time at which failure occurred.

reached could be due to a calibration error in the equipment occurring due to the installation process of the sensors. A locally high void ratio around the sensor, or locally large cracks due to the augering process could account for more rainwater infiltrating the soil than normally possible during high intensity, short duration events. This also explains why the model does not fully capture the increase in water content between an elapsed time of 400 and 500 hours (referring to Figure 4). The discrepancy between the drying paths is likely due to an incorrectly modelled SWCC (which could also be a contributing factor as to why the water content level in the FEM differs to that recorded during the field monitoring). The hysteresis pattern present in the SWCC was not incorporated into the present modelling, and hence could explain the discrepancy between the two drying paths. To obtain a good comparison between the field-measured θ_w and the FEM-calculated θ_w, the empirically obtained SWCC for the soil required adjustments. In particular, the air-entry value has a major influence on the fluctuating water content obtained from the FEM, but the effect of this seemed to be relative to the saturated permeability of the soil. Hence in order to ensure this modelling is correct, laboratory tests such as the pressure plate test and falling head test will be undertaken.

The 2008 hourly rainfall record, as shown in the upper graph of Figure 5, was then applied to this finite element model and limit equilibrium analyses were undertaken at each time step. The factor of safety (FOS) obtained from the 2008 rainfall plotted against time is shown in the lower graph of Figure 5. At each significant rainfall event, there is a sudden decrease in the factor of safety. Following the rainfall event, the FOS begins to gradually recover. The FOS however had no time to recover from the heavy rainfall patterns leading up to the time of the landslide. As seen, the factor of safety reaches a minimum of approximately 1.08 at the same time at which the landslide occurred (late June). This indicates that the finite element model and the limit equilibrium analyses are reasonably calibrated to simulate the observations made at the site. It is anticipated that further laboratory tests to confirm the SWCC and the shear strength of the soil will increase the accuracy of these models. A better estimate of the shear strength and SWCC of the soil layers will also better our understanding of other assumptions made in the analyses. For example, the counterfort drains were assumed to be ineffective due to the low permeability of the soil, and the derelict condition of the pipes. However, field evidence suggests that these drains are still draining away a

reasonable amount of groundwater following a significant rainfall event. It is considered that until reasonable confidence of the soil parameters is achieved, modelling such complexities as the counterfort drains could hide the true response of the slope during rainfall events.

This research is part of a larger project in which a site specific warning system for rainfall induced landslides is being developed. It is envisioned that using a fully verified FEM-based approach and limit equilibrium analyses, a database of the water content profiles, and their corresponding factors of safety will be developed. Then during rainfall events, the water content profile at the site can be obtained from the water content sensors. These water contents can be compared with those in the database, and the factor of safety estimated from those in the database with similar water contents, thus providing the user with an estimated factor of safety against slope failure. The user can then take any necessary action, such as lowing speed limits or closing roads.

5 CONCLUSIONS

Slope monitoring and numerical analyses were conducted at a site where rainfall-induced slope failure occurred during the winter of 2008. The fluctuating field-measured θ_w during 2010 was replicated in a FEM using soil-water relationships obtained based on empirical methods. There was small discrepancy between the field measured and FEM-calculated water contents, particularly during the drying path of the soil. This can be attributed to the empirical relationship used to derive the SWCCs. Next, the known rainfall pattern which caused slope failure in 2008 was applied as an influx to the model and a limit equilibrium analysis was undertaken at each time step to determine the factor of safety corresponding to each rainfall event. As the factor of safety reached a minimum of 1.08 at approximately the same time as when the landslide occurred, it was concluded that the model was in near-calibration. The accuracy of this model will be further improved using laboratory tests to confirm the SWCCs and shear strength relationships, which were estimated using empirical procedures. It was aimed that once the model is fully calibrated; it can be used to develop a site-specific warning system.

ACKNOWLEDGEMENTS

The authors wish to thank the National Institute of Occupational Safety and Health, Japan for funding this project. Also thanks to Hiway Geotechnical, Babbage Consultants, the Auckland Motorways Alliance (AMA) and Beca Consultants for their assistance with the project.

REFERENCES

Arya, L. M., Leij, F. J., van Genuchten, M. T. & Shouse, P. J. (1999). Scaling parameter to predict the soil water characteristic from particle-size distribution data. *Soil Science Society of America Journal, 63*, 510-519.

Arya, L. M. & Paris, J. F. (1981). A Physicoempirical model to predict the soil moisture characteristic from particle-size distribution and bulk density data. *Soil Science Society of America Journal, 45*, 1023-1030.

Arya, L. M., Richter, J. C. & Davidson, S. A. (1982). A comparison of soil moisture characteristic predicted by the Arya-Paris with laboratory-measured data. *AgRISTARS Tech. Rep. SM-L1-04247, JSC-17820*, NASA-Johnson Space Centre

Brooks, S. M., Crozier, M. J., Preston, N. J. & Anderson, M. G. (2002). Regolith stripping and the control of shallow translational hillslope failure: application of a two-dimensional coupled soil hydrology-slope stability model, Hawke's Bay, New Zealand. *Geomorphology, 45*, 165-179.

Hawke, R. & McConchie, J. (2011). In situ measurement of soil moisture and pore-water pressures in an 'incipient' landslide: Lake Tutira, New Zealand. *Journal of Environmental Management, 92*(2), 266-274.

NIWA & G.N.S. (2009). *Natural Hazards 2008*.

O'Sullivan, A. S. (2009). Suitability of advanced soil models for stability analysis of slopes in Northland soils. *Masters Thesis,* The University of Auckland, Auckland.

Tilsley, S. C. (1998). *PA 1651 Investigation, Design & Supervision for State Highway 1 - Albany to Puhoi Realignment (ALPURT) Sector B1 - Silverdale to Orewa*: Beca Carter Hollings & Ferner Ltd.

van Genuchten, M. T. (1980). A closed-form equation for predicting the hydraulic conductivity of unsaturated soils. *Soil Science Society of America Journal, 44*(5), 892-898.

Vanapalli, S. K., Fredlund, D. G., Pufahl, D. E. & Clifton, A. W. (1996). Model for the prediction of shear strength with respect to soil suction. *Canadian Geotechnical Journal, 33*(3), 379-392.

Winkler, G. E. (2003). The geology of the Northland Allochthon. *Geotechnics on the Volcanic Edge Conference* Tauranga, New Zealand.

Zhan, L. T., Ng, C. W. W. & Fredlund, D. G. (2007). Field study of rainfall infiltration into a grassed unsaturated expansive soil slope. *Canadian Geotechnical Journal, 44*, 392-408.

明かり掘削における掘削面の勾配と高さの基準制定に至る歴史的背景

(独)労働安全衛生総合研究所　○国際　伊藤和也，国際　豊澤康男
元　労働省産業安全研究所　正　前郁夫
東京工業大学　国際　高橋章浩，国際　竹村次朗，国際　日下部治

Keywords: 掘削勾配，掘削高さ，労働安全

1.　はじめに

掘削工事における労働災害の大部分は，土砂崩壊による災害である．その防止対策の重要性は古くから認識されており，1965（昭和40）年の労働安全衛生規則の一部を改正する省令において，掘削面の勾配と高さの基準等が定められ，現在に至るまで引き継がれている（表-1）．本報では，掘削面の勾配と高さの基準である労働安全衛生規則第356条・357条について，制定された歴史的背景の調査を行い，また理論的背景についても幾つかの数値解析手法により考察を行った．

2.　掘削面の勾配と高さの基準の歴史的背景

掘削面の勾配と高さの基準の歴史的背景，特にどのように勾配と高さを決定したかについて，当時を知る複数の関係者から聞き取り調査を行った．この決定根拠としては大きく2つの理由があるようである．1点目は，1959（昭和34）年労働基準局長通達（昭和34年5月15日基発第367号）により高さ2m以上の法面下作業について，緻密な岩盤及び堅硬な粘土を除いて75度を超えない勾配の基準とするように指導を行っていたことである．2点目は，過去の災害事例の掘削面の勾配と高さについて調査したことである．具体的には，1959（昭和34）年5月発行の安全資料「土砂崩壊災害の防止」[1]内に記載されている1954（昭和29）年～1958（昭和33）に発生した土砂崩壊による重大災害64件（死傷者数283名，うち死亡者数132名）および岩石崩壊落下による重大災害23件（死傷者数123名，うち死亡者数50名）から掘削面の勾配と高さが記載された24件の災害事例の掘削面の勾配と高さの分布を参考にして決定している．図-1は文献から筆者らが抽出した24件の災害事例の分布に労働安全衛生規則第356条での基準を併記したものである．以上の2つの理由より掘削面の勾配と高さは総合的に決定されたものと考えられる．最低限遵守すべき基準として現在まで変更されずにいることからも，制定に携わった当時の技術者の見識の高さが伺える．

3.　掘削面の勾配と高さの基準の理論的背景

上述のように掘削面の勾配と高さの基準は，基本的には制定前に存在した通達と災害事例データから決定されたが，同時に理論的な検討もなされていた．安全資料「土砂崩壊災害の防止」には，直線すべり法にて粘土の切取限界高さを計算した結果が示されている．当時の土質力学の書籍「土質力學」[2]（1951（昭和26）年発行）では，“12章　法面の安定”にてTaylorの安定図表等が示されている．これらの検討は全て円弧すべり法によるものであったが，災害による崩壊形状では円弧すべりは極僅かであり，そのほとんどが直線すべりであったことから安全資料では直線すべり法による計算が採用されている．

表-1　労働安全衛生規則　第356条・第357条

	地山の種類	掘削面の高さ（単位　m）	掘削面の勾配（単位　度）
356	岩盤又は堅い粘土からなる地山	5未満	90
		5以上	75
	その他の地山	2未満	90
		2以上5未満	75
		5以上	60
357	砂からなる地山	勾配35度以下又は掘削面の高さ5m未満	
	発破等の後の地山	勾配45度以下又は掘削面の高さ2m未満	

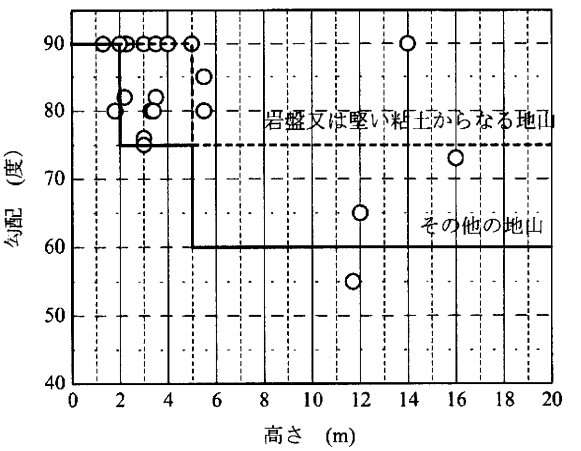

図-1　災害事例における掘削面の勾配と高さの関係と労働安全衛生規則第356条の比較

4.　数値解析による検討

労働安全衛生規則の検討にも利用された「直線すべり法」に加えて，「剛塑性有限要素法」を用いてすべり線形状などについて比較・検討を行った．剛塑性有限要素法はTamura et. al[3]の開発したプログラムを利用し，外力として自重を0から少しずつ増加させて崩壊時の重力加速度を求める“重力加速度増加手法”を用いた。

図-2に2種類の数値解析結果とChenらの安定係数[4]を示す．なお，凡例の数字は内部摩擦角である．直線すべり法（図-2(a)）では，勾配が90度ではChenらの安定係数と近い値を示しているが，その他の勾配では直線すべりの安定係数が大幅に上回っている．緩勾配のケースほどその差は広がった。一方，剛塑性有限要素法（図-2(b)）では，Chenらの安定係数に近い傾向を示した．若干剛塑性有限

The historical and theoretical background of enacting standards for the gradient of excavation surfaces
K. Itoh, and Y. Toyosawa (National Institute of Occupational Safety and Health, Japan), I. Mae (Former National Institute of Industrial Safety, Ministry of Labour), A. Takahashi, J. Takemura, and O. Kusakabe (Tokyo Institute of Technology)

要素法の安定係数が大きな値を示しているが，これは，剛塑性有限要素法の収束判定による誤差の影響だと考えられる．

剛塑性有限要素法より得られた相当塑性ひずみ速度分布の一覧を表-2 に示す．この表には，直線すべり法にて得られるすべり線勾配も赤色点線で一緒に図示した．内部摩擦角が小さい，すなわち粘性土地盤のケースでは，崩壊形状が円弧状となっており，直線すべり法によるすべり線勾配とは全く異なる．しかし，内部摩擦角が大きい，すなわち砂質土地盤では，崩壊形状が表層部分に集中し，直線すべり法によるすべり線と合致する．また，勾配の違いで見ると，急勾配ほどすべり線形状は内部摩擦角が小さい場合でも直線となる傾向が見られた．直線すべり法では，このようなすべり線の違いが安定係数にも大きな影響を与えたものと想像される．しかし，急勾配掘削において簡易的に安定係数を求める場合には，直線すべり法でも大きな差とはならないとも言える．

5. まとめ

本報では，仮設時に最低限遵守すべき基準である労働安全衛生規則について，制定された歴史的背景の調査および理論的背景について検討を行った．以下に得られた知見を示す．

1. 労働安全衛生規則第356条および第357条の掘削面の勾配と高さの基準は，制定前に存在した通達と災害事例データから決定された．しかし，それ以外にも直線すべり法による数値解析なども行って理論的な検討もされていた．当時の土質力学はまだまだ未成熟な時代であったが，当時の最先端の知見を取り入れて制定されたと言える．
2. 直線すべり法による結果は急勾配掘削の場合には，剛塑性有限要素法の崩壊形状とも良い整合を示していることから，急勾配掘削において簡易的に安定係数を求める場合には，直線すべり法でも大きな差とはならないといえる．

謝辞

本報をまとめるにあたり，加来利一氏（前 労働省安全衛生部長）から貴重な情報と有益なご助言を戴きました．ここに深謝の意を表します．

本研究は，厚生労働省科学研究費補助金（労働安全衛生総合研究事業 課題番号H20-労働-一般-001，代表研究者：日下部治）の補助を受けた．ここに記して謝意を表する．

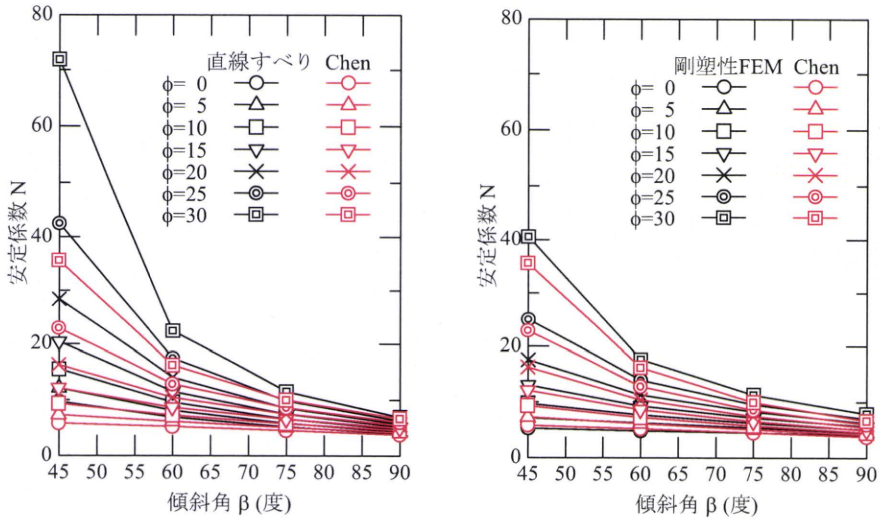

(a) 直線すべり　　(b) 剛塑性 FEM

図-2 Chen らの安定係数との比較

表-2 剛塑性 FEM での相当塑性ひずみ速度分布と直線すべり法でのすべり線

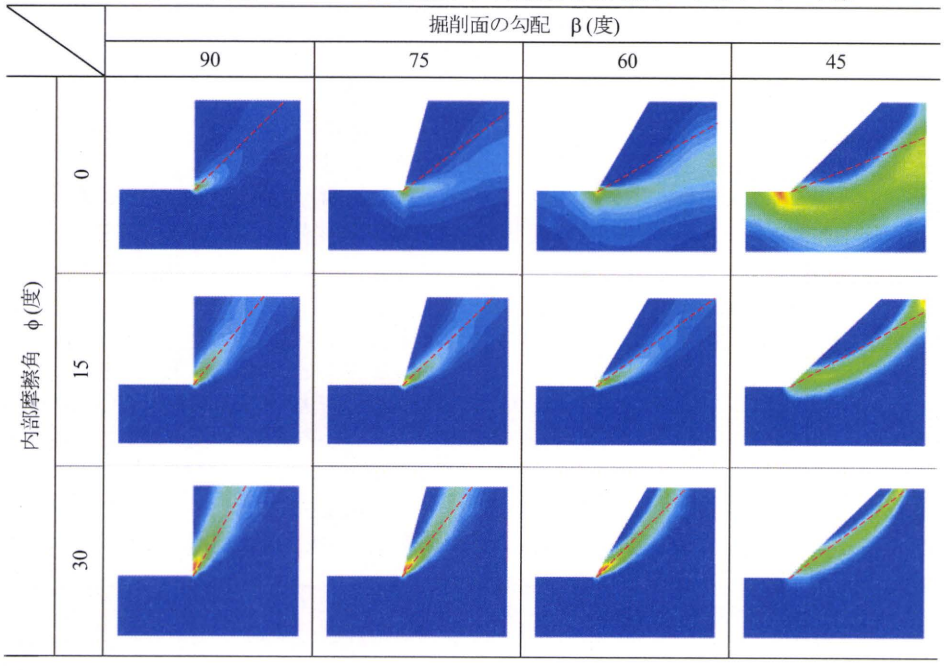

参考文献

1) 労働省労働基準局安全課：安全資料 (B-5)「土砂崩壊災害の防止」，pp.130-136，1959
2) 最上武雄：第 12 章 法面の安定，土質力學，岩波全書 148，pp.166-172，1951.
3) Tamura, T., Kobayashi, S. and Sumi, T. : Limit analysis of soil structure by rigid plastic finite element method, Soils and Foundations, Vol. 24, No. 1, pp.34-42, 1984.
4) Chen, W. F., Giger, M. W., and Fang, H. Y. : On the limit analysis of stability of slopes, Soil and foundations, Vol. 9, No. 4, pp.23-32, 1969.